Experimental Investigation of Pulsed Thrust Performance for Underwater Propellers

Dev Dalmia, Jet Sherman, Luke Harris, Ronan Wang

Background and Motivation

Why underwater vehicles and motor pulsing?

Unmanned underwater systems have a wide variety of uses across environmental research, coastal security, infrastructure maintenance and deep-sea exploration. These UUVs are generally powered by propeller systems. Mostly operating in a steady state, the transient pulsing of these propellers also has potential applications:

1. Do deep water or long range applications/missions. Strict energy constraints demand efficiency to increase mission scope, range, and reliability.

2. Low power bursts allow position keeping against ocean currents, wakes, and tides to keep the UUV at a fixed position.

3. UUVs need to generate thrust quickly for greater accuracy in position keeping as well as reducing mechanical wear and motor stress due from torque demands in the transient regime.

Figure 1: Boxfish robotics AUV for deepsea scientific research

Application in Monitoring Hydrothermal Vents

UUVs are currently used sample thermal and chemical pools above hydrothermal vents deep underwater.

1. The chemical composition of these vents are directly related to the understanding and monitoring of earthquake and volcanic activity around the world.

2. Research missions can take 12+ hours such as the Woods Hole Institute Pacific Vent study in 2024 where 5 new hydrothermal vents were discovered.

3. High precision UUV control is needed to record data from vents that can occur at depths between 7,000 and 8,250 feet but at times have diameters of just a few centimeter.

4. Here, accurate and high performance position keeping is a crucial marker of UUV performance. Propeller choice will directly impact the duration and quality of vent sampling.

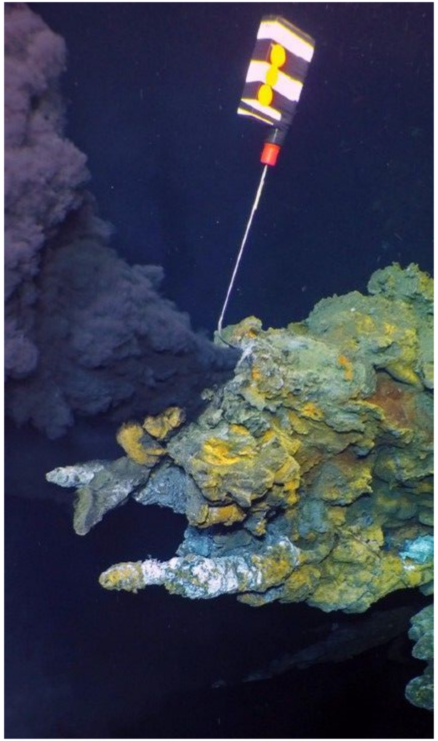

Figure 2: UUV Monitoring a Hydrothermal Vent in the Pacific

Premise

- Our Goal: Test the efficiency of common UUV propellers in the transient regime.
- We picked four common propeller types to see how their design affects transient performance.
- First, we looked at previously researched steady state open-water efficiency of these propellers. Then compared to our experimental results in the static regime at both steady and transient speeds.

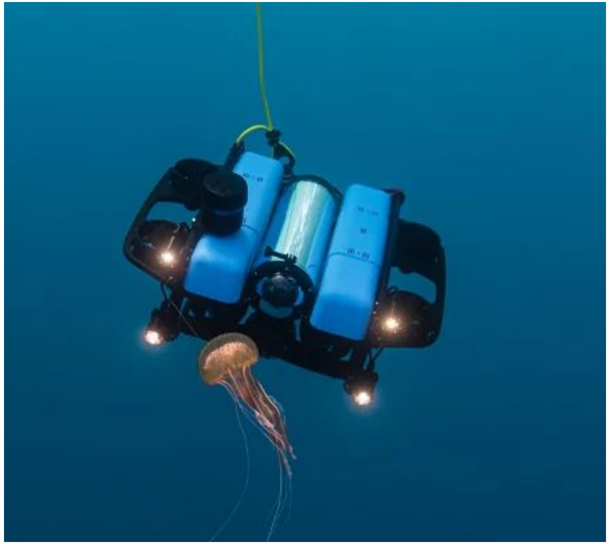

Figure 3: LA-Based Blue Robotics BlueROV2 used for underwater research driven by a six propeller setup

Theoretical Background

Propeller Efficiency in the Transient Region: currently no closed-form thrust equation.

Propeller Efficiency in Open Water: Defined by the "Wageningen B-Series data" (University of Michigan 1981), widely used in Naval Architecture. 120 propellers tested and recorded to produce accurate empirical data for a wide range of propeller geometries and applications.

K_T (Thrust Coefficient) and K_Q (Torque Coefficient) describe how efficiently a propeller converts rotational speed into thrust and torque. These are derived from blade area, pitch-to-diameter ratio, advance ratio (J), and blade number (Z).

$$K_T = \sum_i C^{(T)}_{s,t,u,v} \; J^{\,s} \cdot \left(\frac{P}{D}\right)^t \cdot \left(\frac{A_E}{A_0}\right)^u \cdot Z^{\,v}$$

$$K_Q = \sum_i C^{(Q)}_{s,t,u,v} \; J^{\,s} \cdot \left(\frac{P}{D}\right)^t \cdot \left(\frac{A_E}{A_0}\right)^u \cdot Z^{\,v}$$

$$\eta = \frac{J \cdot K_T}{2\pi \cdot K_Q}$$

Advance Ratio J: relates vehicle speed to propeller speed. V_a is the advance velocity, n is revolutions per second and D is the propeller diameter. However, in static operation (experienced during pulsed position keeping) J = 0 as thrust is produce from stagnant or close to stagnant flow.

$$J = \frac{V_a}{n\,D}$$

Measuring Efficiency: A fixed motor system makes it impossible to generate an efficiency value due to static conditions. Instead, compare input electrical power to thrust generation using the “Power Loading” equation characterized by NASA’s Hover Efficiency study.

$$\frac{T}{P} = \frac{T}{V \cdot I} \qquad [\mathrm{N/W}] \text{ or } [\mathrm{gf/W}]$$

Wageningen B-Series Propeller Constants

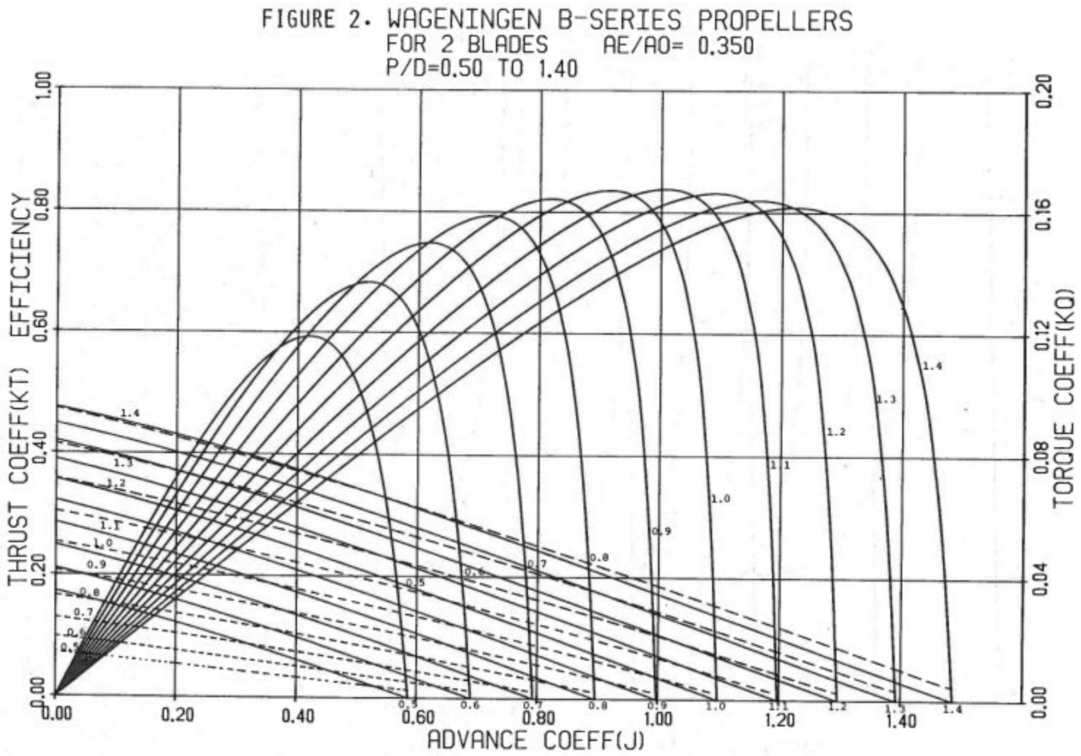

Figure 4: Coefficient of Torque and Thrust chart based on propeller characteristics and advance ratio

Theoretical Efficiency Input Values

Propeller	Diameter (D)	Blade Count (Z)	P/D	Ae/Ao	J	K_T	K_Q
Graupner 455/9	50mm	2-Blade	1.0	0.454	0.40	0.253	0.047
Graupner 2303/50	50mm	2-Blade	0.84	0.331	0.40	0.158	0.020
Graupner 2313/2	50mm	3-Blade	1.19	0.52	0.40	0.365	0.085
Graupner 2305/50	50mm	2-Blade	1.6	0.454	0.40	0.530	0.165

Table 1: Our propeller geometry and efficiency coefficients at an estimated open-water, low-speed UUV conditions. Wageningen B-Series models are used to assume efficiency in open water conditions.

Selected Propellers

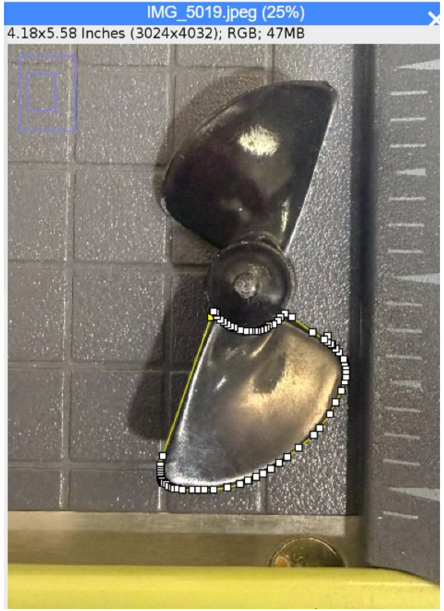

Figure 5: Graupner 2303/50

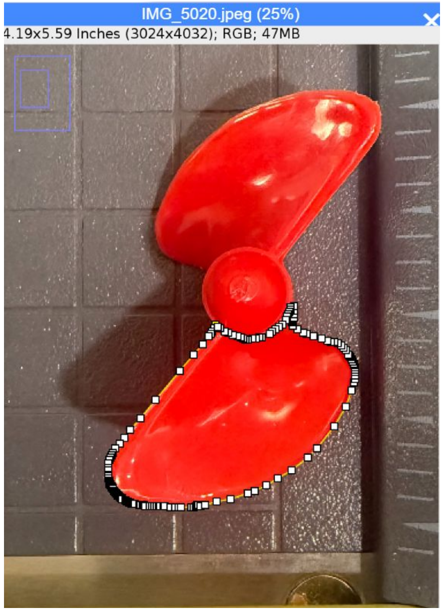

Figure 6: Graupner 455/9

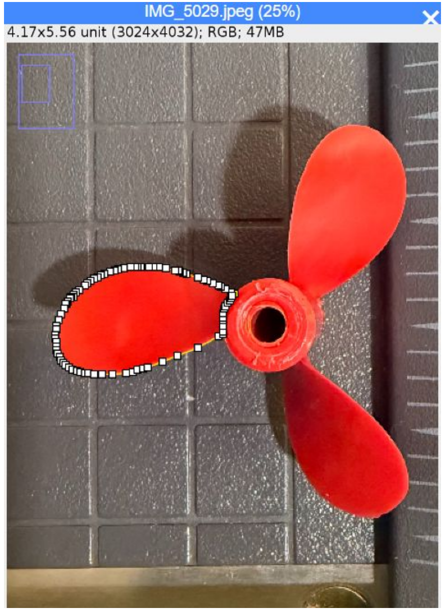

Figure 7: Graupner 2313/2

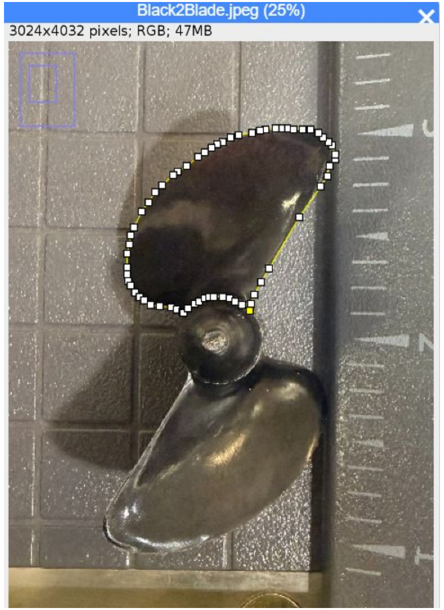

Figure 8: Graupner 2305/50

ImageJ software was used to calculate approximate blade area (planform area) using ruler and constant camera placement.

Predictions + Hypothesis

Theoretical K_Q and K_T

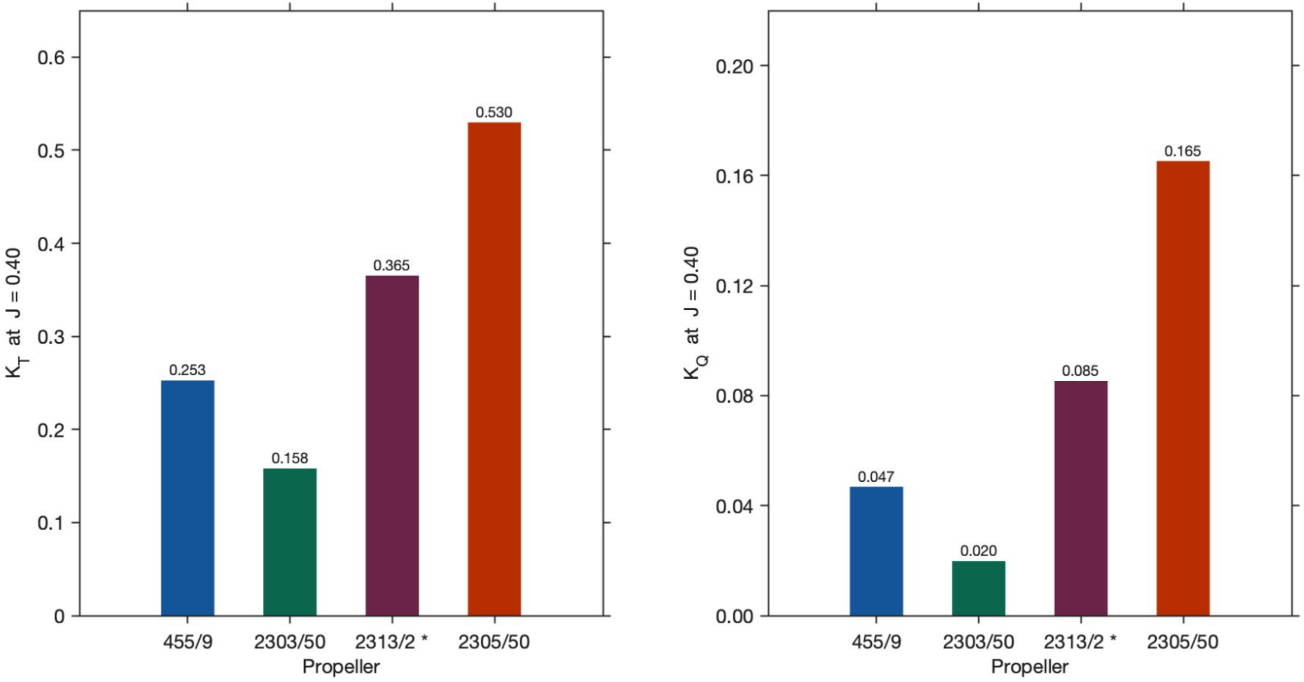

Figure 9: Wageningen B thrust and torque coefficients of the four propellers

Key Notes:

- Pitch/Diameter Ratio positively correlated to thrust at 0-1500 RPM.
- Geometric changes such as Ae/Ao.
- At RPM lower than 200, thrust generation across designs are very similar

Model Prediction of Propellers in the Sub 2000 RPM Regime

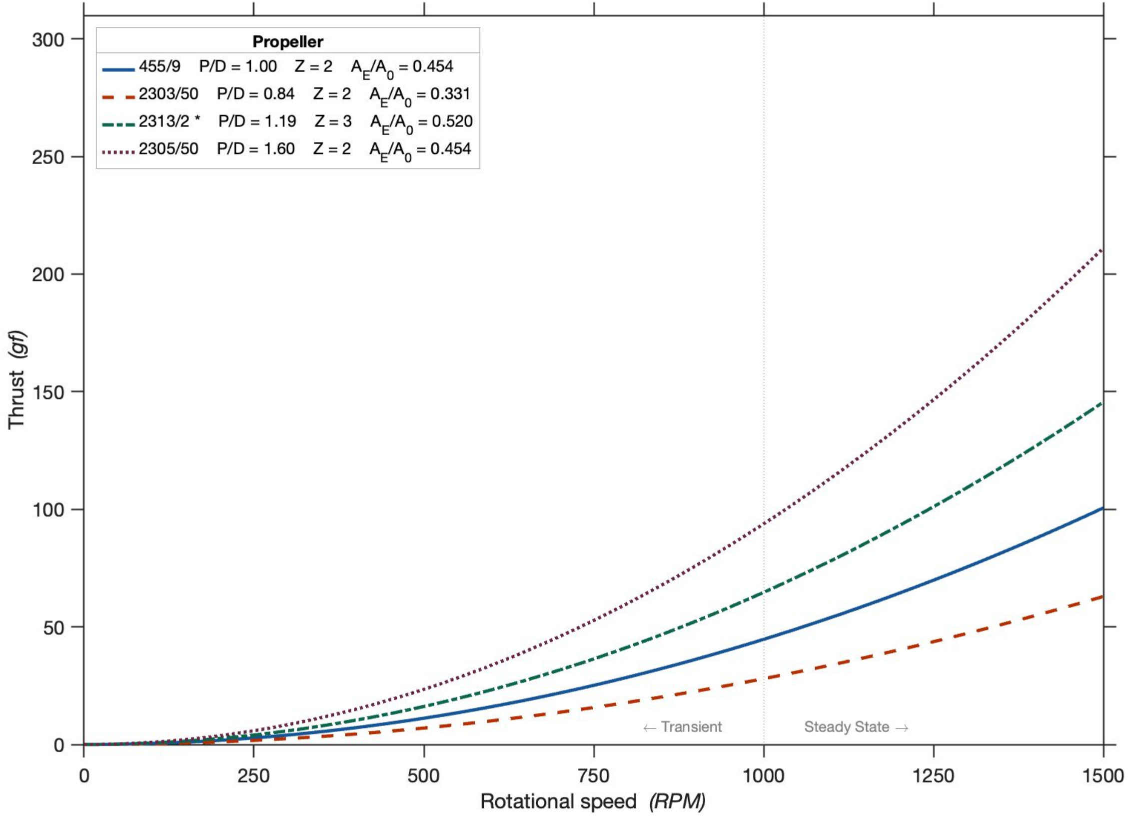

Figure 10: Wageningen Bthrust approximation of our four propellers between 0-1500 RPM

Key Notes:

- Pitch/Diameter Ratio positively correlated to thrust at 0-1500 RPM.
- At RPM lower than 200, thrust generation across designs are very similar.

Theoretical Efficiency

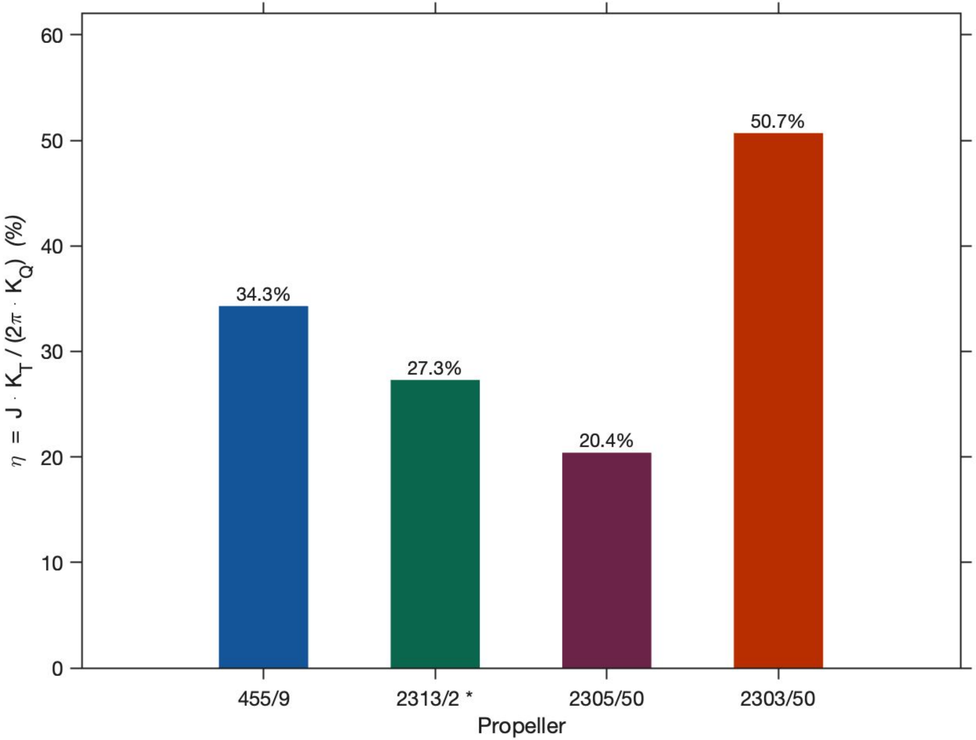

Figure 11: Wageningen B Efficiency approximation of our four propellers at an Advance Ratio of J=0.40

Key Notes:

- P/D drives efficiency (2303/50 lowest P/D)
- The 3-blade (2313/2) penalty. Despite a moderate P/D of 1.19, the extra blade inflates both KT and KQ significantly pulling efficiency down to 27.3%.
- At a low J, power is too low to take advantage of the high P/D of 2305/50.

Materials and Methods

Experimental Setup Potential Issues

Safety Concerns: With a water tank involved, the experiment was moved outside to reduce electrical risks. An extended shaft was used to keep only the propeller in the water.

$$f_1 = \frac{\beta_1^2}{2\pi L^2}\sqrt{\frac{EI}{\rho A}} \qquad \beta_1 = 1.875$$

$$f_1 = \frac{(1.875)^2}{2\pi(0.300)^2}\sqrt{\frac{(193\times 10^9)(1.26\times 10^{-11})}{(8000)(1.26\times 10^{-5})}} \approx 30.5\text{ Hz}$$

Vibration Analysis: With an extended shaft, ensuring that our system would be free of resonance was crucial. We calculated using the expected characteristics of our setup.

$$f_{\text{BPF}} = B \cdot \frac{\text{RPM}}{60}$$

Configuration	Formula	Result
2-blade	$2\times\frac{1500}{60}$	50 Hz
3-blade	$3\times\frac{1500}{60}$	75 Hz

Measurement Sensitivity: Thrust generation estimated to be approximately 200 grams based on a median Kt value (0.5) and RPM (1500) from our motor specifications. These values informed our choice of a 1kg load cell to accurately capture the thrust output.

$$T = \rho\, n^2\, D^4\, K_T$$

$$T = (1000)(25^2)(0.05^4)(0.5)$$

$$= (1000)(625)(6.25\times 10^{-6})(0.5)$$

$$\approx 1.95\text{ N} \approx 199\text{ gf}$$

Wall Effect Mitigation

Wall Effects: A large concern when testing water flow not in a large body of water. We selected an appropriate water container which satisfied dimensions suggested by literature

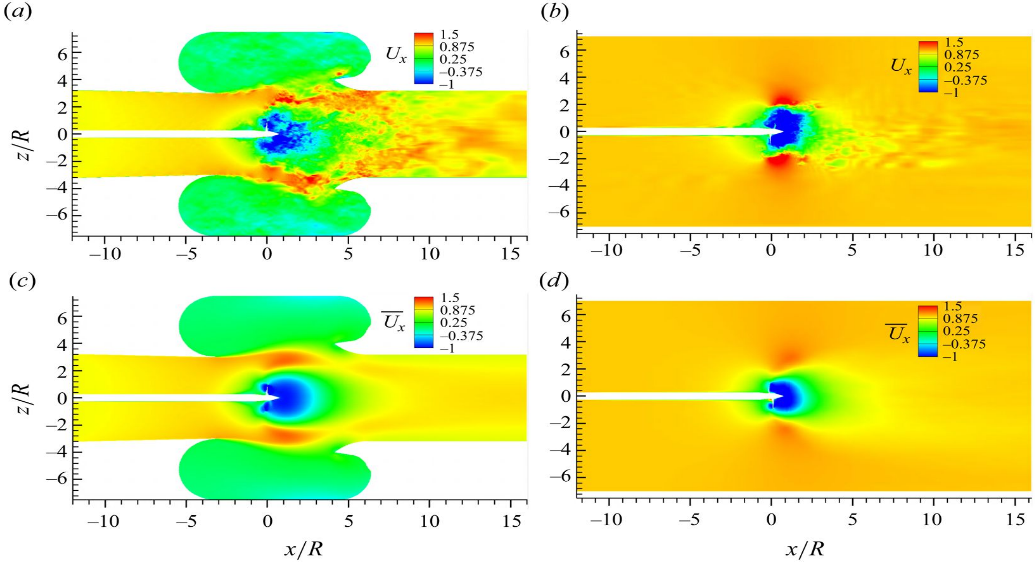

$$\eta = \frac{A_{\text{prop}}}{A_{\text{tank}}} \ll 1$$

$$A_{\text{prop}} = \pi(0.025)^2 = 1{,}963 \text{ mm}^2$$

$$A_{\text{tank}} = 685 \times 559 = 383{,}115 \text{ mm}^2$$

$$\eta = 1963 \ / \ 383{,}115 = \mathbf{0.0051} \ll 1 \ \checkmark$$

Figure 12. Instantaneous (a, b) and time-averaged (c, d) axial velocity contours U_x/U_∞ comparing a confined Variable Pressure Water Tunnel (VPWT, left column) to open water conditions (OW, right column) at $J = -0.82$. Spatial axes normalised by propeller radius R.

Posa, A., Balaras, E., & Broglia, R. (2022). A large-eddy simulation study of water tunnel interference effects for a marine propeller in crashback mode of operation. *Journal of Fluid Mechanics*. Cambridge University Press.

Experimental Setup

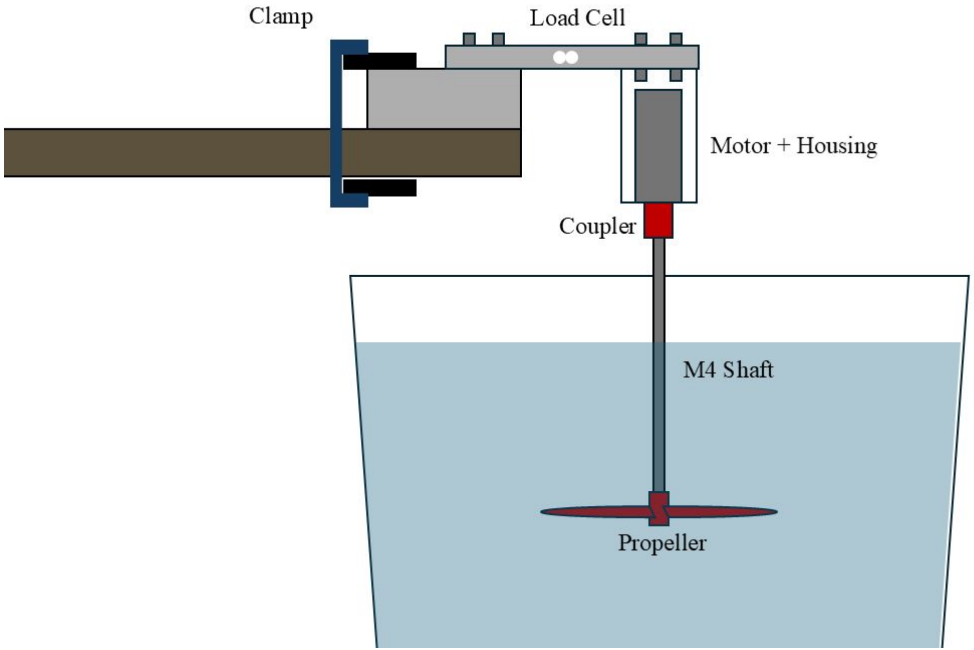

Figure 13: Experimental setup assembled outside lab on the edge of a desk

- Load cell clamped to table on one end and fixed to motor on other.
- Coupler connecting motor shown to M4 threaded rod with propeller on the end.
- Propeller placed the appropriate distance below the surface of the water to avoid unwanted effects.

Physical Setup

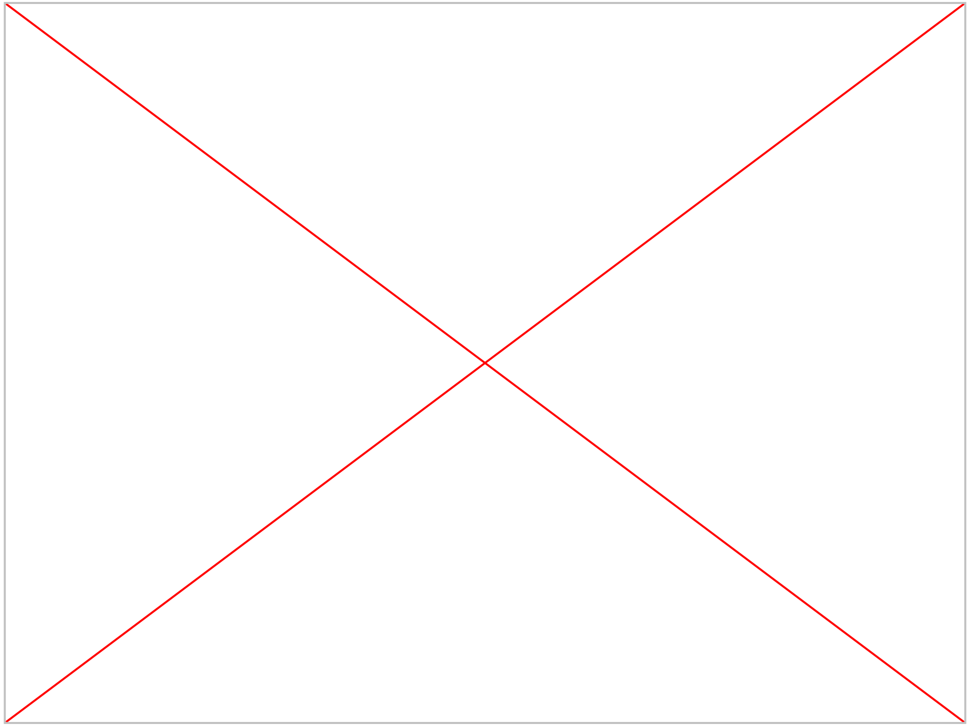

Figure 14: Video of Experimental setup from lab 4/28/2026

- Table was stabilized against vibrations using PVC pipes.
- Thrust generation pushed flow downward into tank.
- Electrical Power read off the DC Power Supply for each trial.

Differential Amplifier

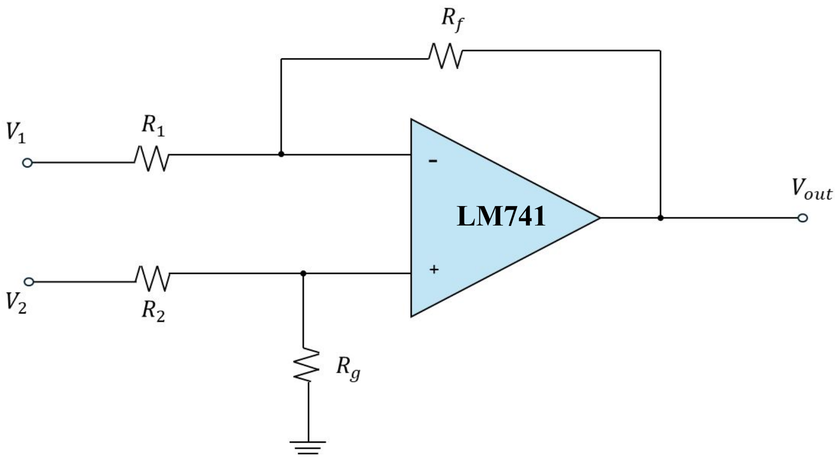

Figure 15: Differential Op-Amp circuit features four different resistors, which can be manipulated to give an easily calculated voltage gain

$$R_1 = R_2$$
$$R_f = R_g$$
$$\longrightarrow \quad V_{out} = \frac{R_f}{R_1}(V_2 - V_1)$$

Advantages of Differential Op-Amp Circuit

1. Common-mode noise rejection
2. Resistor choice decides gain
3. Allows for high signal to noise ratios

Wiring and Procedure

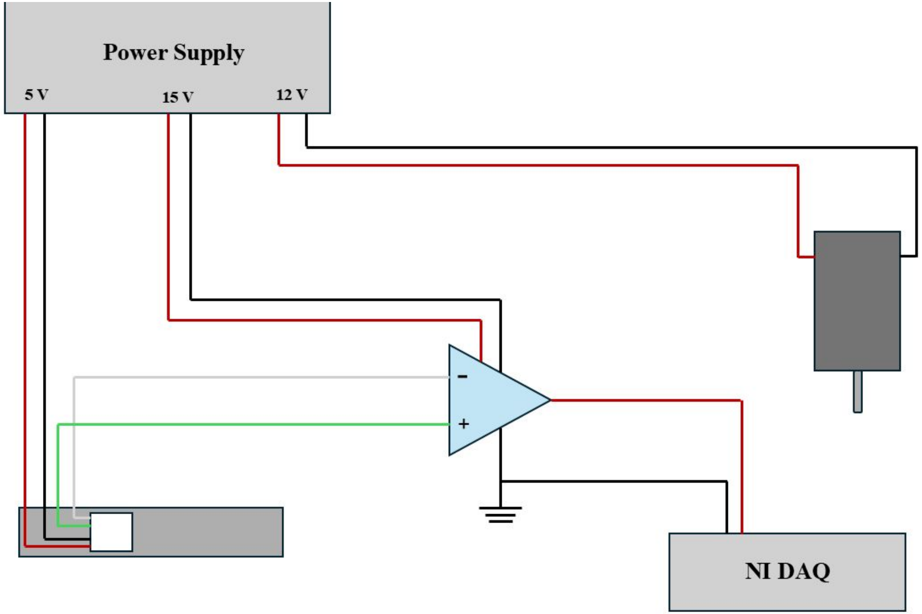

Figure 16. Simple wiring diagram showing how all electronic components are connected for motor control and data acquisition

Procedure

1. Start VI for data collection and wait approximately 1 second
2. Turn on 12V power supply port connected to DC motor
3. Let motor run until the VI stops and turn off motor
4. Inspect time trace to ensure transient region reasonably captured

Repeat for 5 trials with each propeller so that reasonable uncertainties can be calculated

Load Cell Calibration

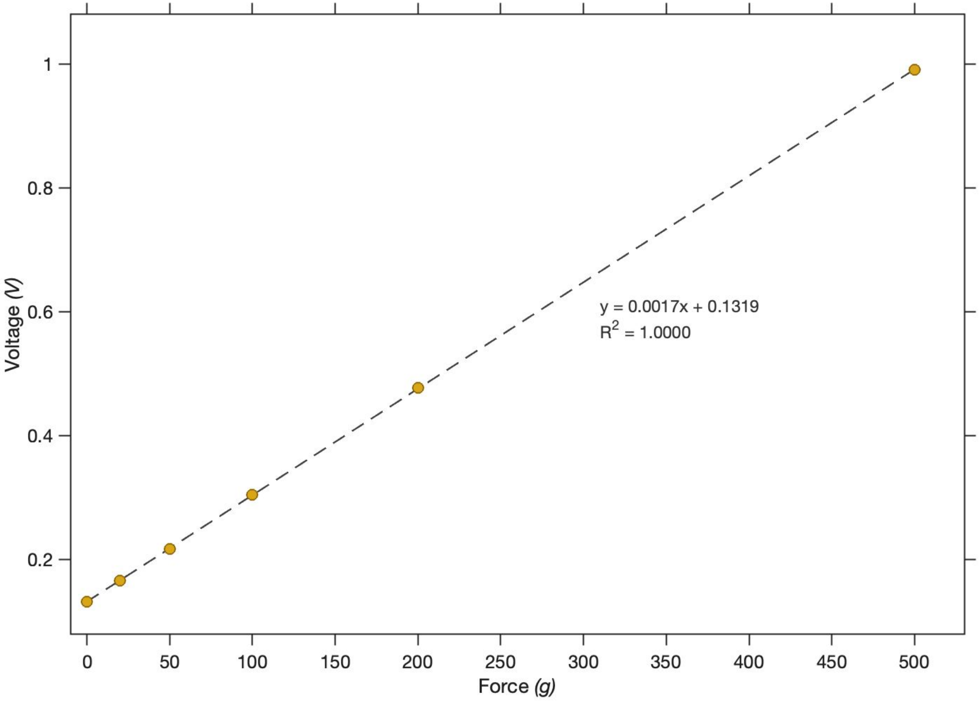

Figure 17: Calibration curve shows very strong linear relationship

- Measurements taken at six different known weights across the entire expected range
- Calibration curve shows proof of linearity well past expected maximum thrust force
- Offset not important as it will change when apparatus is fully assembled
- Calibration constant of 0.0017 with an $R^2 = 1$

Results

Data Analysis Process

Initial Data Processing in MATLAB

- Data zeroed by averaging first 2000 samples to use as y-intercept of the voltage-gram conversion factor.
- Motor power found using “detectTurnOn(*v*)”. *v* is 25 a point average if its derivative exceeds signal noise.
- All trials aligned starting 2000 points before detected motor turn on and an average was taken at each point.
- The average thrust trace is smoothed using a 15 point moving mean window.

Graph Creation

- A mean representative trace for each propeller is plotted with 95% confidence intervals.
- The “transient” regime impulse is defined as 0-0.2s from motor turn on and “steady state” is 0.2s-2.2s.
- Impulse is compared to power input on final bar graph with error bars.

Error Calculation

- Error calculated using 95% confidence interval with 5 samples per propeller.
- The impulse error is estimated by integrating the confidence band for the data used over transient and steady state.

Representative Thrust Trace

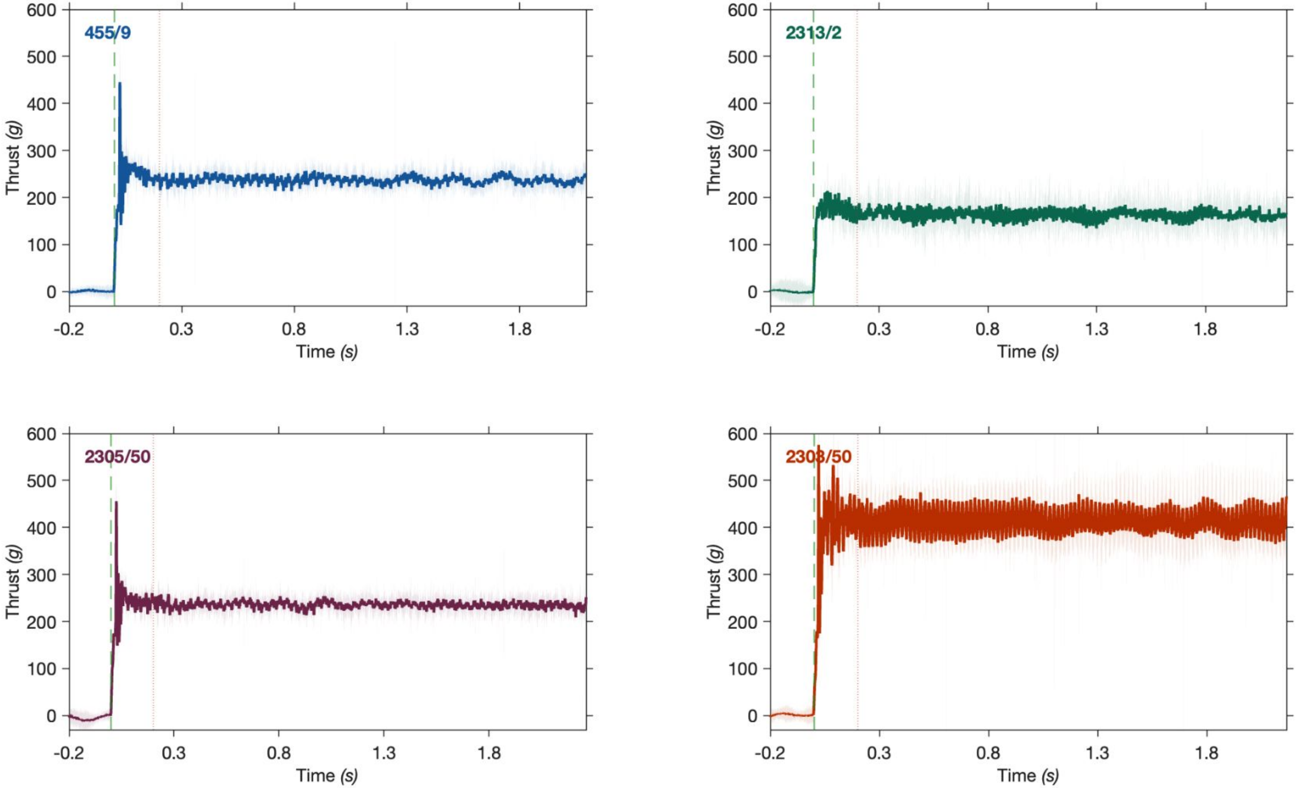

Figure 18: Representative Trace of Mean Thrust for Propellers 455/9 (Blue), 2313/2 (Green), 2305/50 (Purple), and 2305/50 (Orange). 95% Confidence Intervals plotted in background of mean.

Highest Signal noise seen at largest thrust output (2305/50)

Initial spike before steady-state seen on all graphs but 2313/2 (Green) (3 Blade Propeller)

Engine Turn-on denoted with dotted line on left side of trace

Impulse of Thrust In the Steady State Regime

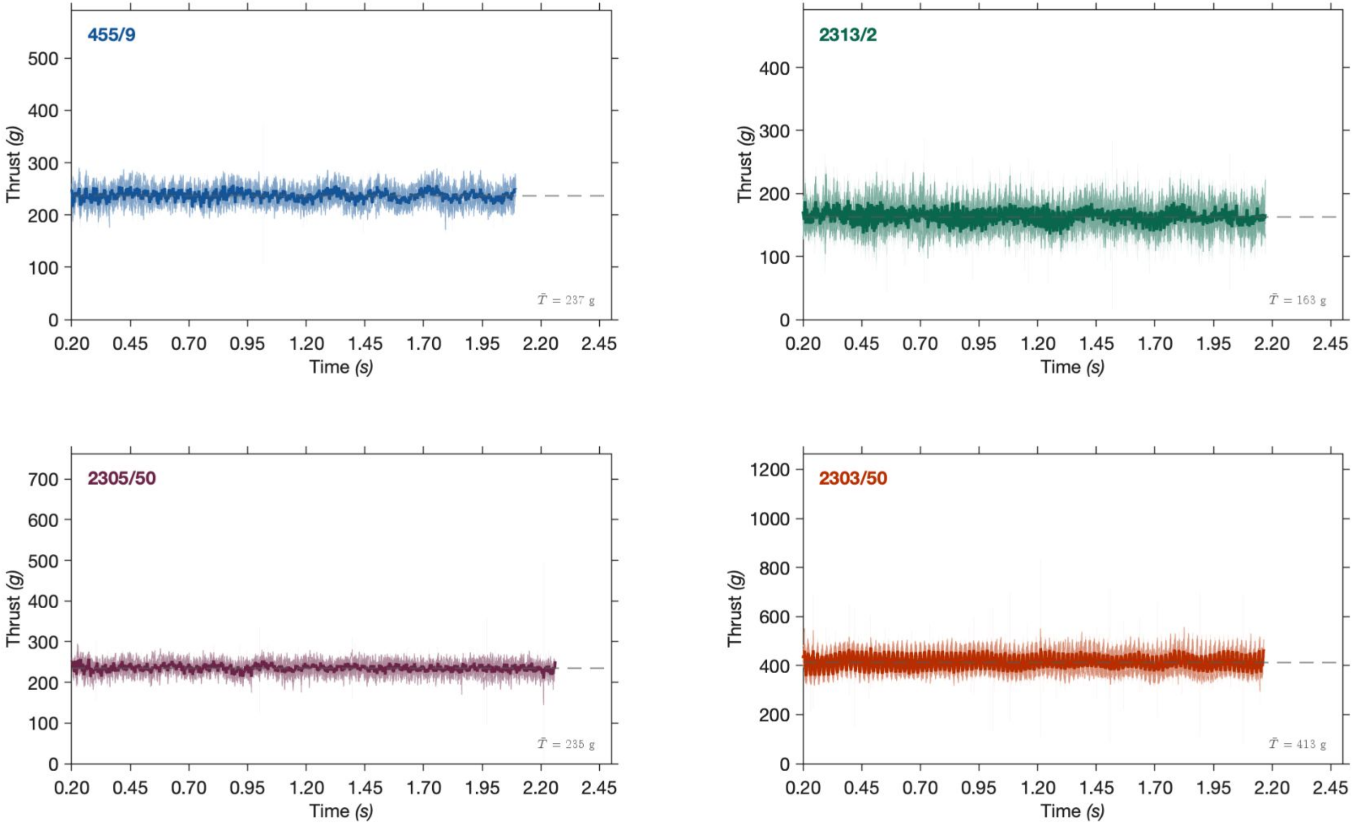

Figure 19: Representative Trace of Mean Thrust for Propellers from through the Steady State Regime. 455/9 (Blue), 2313/2 (Green), 2305/50 (Purple), and 2305/50 (Orange). 95% Confidence Intervals plotted in background of mean

Impulse of Thrust In the Transient Regime

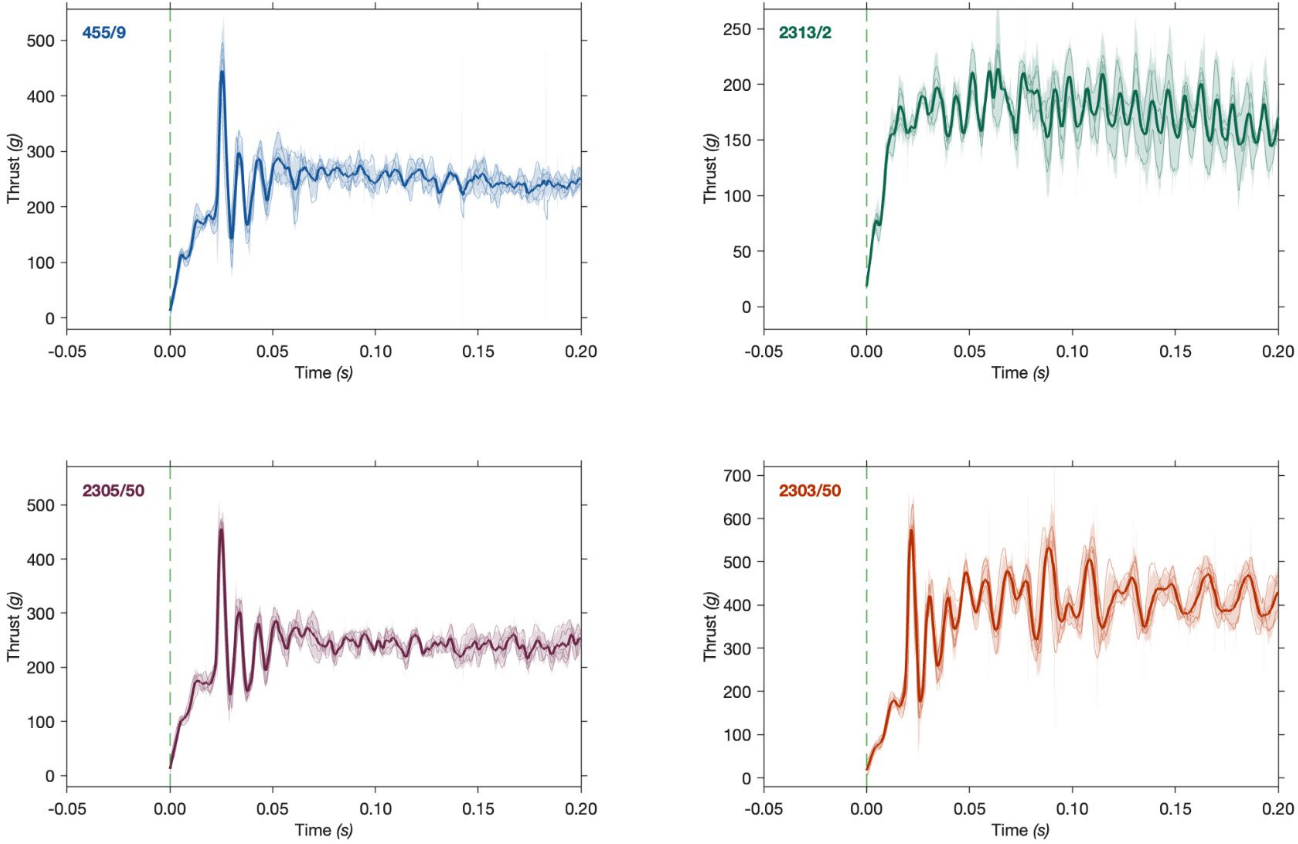

Figure 20: Representative Trace of Mean Thrust for Propellers from through the Transient Regime. 455/9 (Blue), 2313/2 (Green), 2305/50 (Purple), and 2305/50 (Orange). 95% Confidence Intervals plotted in background of mean.

Electrical Input Power

Electrical Input Power	**Voltage Output (Fixed at 3A)**							
Propeller	Trial 1	Trial 2	Trial 3	Trial 4	Trial 5	Average	Power (W)	STD
455/9	7.10	7.11	7.09	7.10	7.12	7.10	21.31	0.010
2313/2	6.64	6.61	6.59	6.65	6.62	6.62	19.87	0.021
2305/50	7.31	7.28	7.33	7.3	7.31	7.31	21.92	0.016
2303/50	8.55	8.56	8.49	8.57	8.54	8.54	25.63	0.028

Table 2: Electrical Power readings read off DC power supply during each trial. Photo was taken of DC power supply to record data in real time.

Impulse Vs. Electrical Input Power

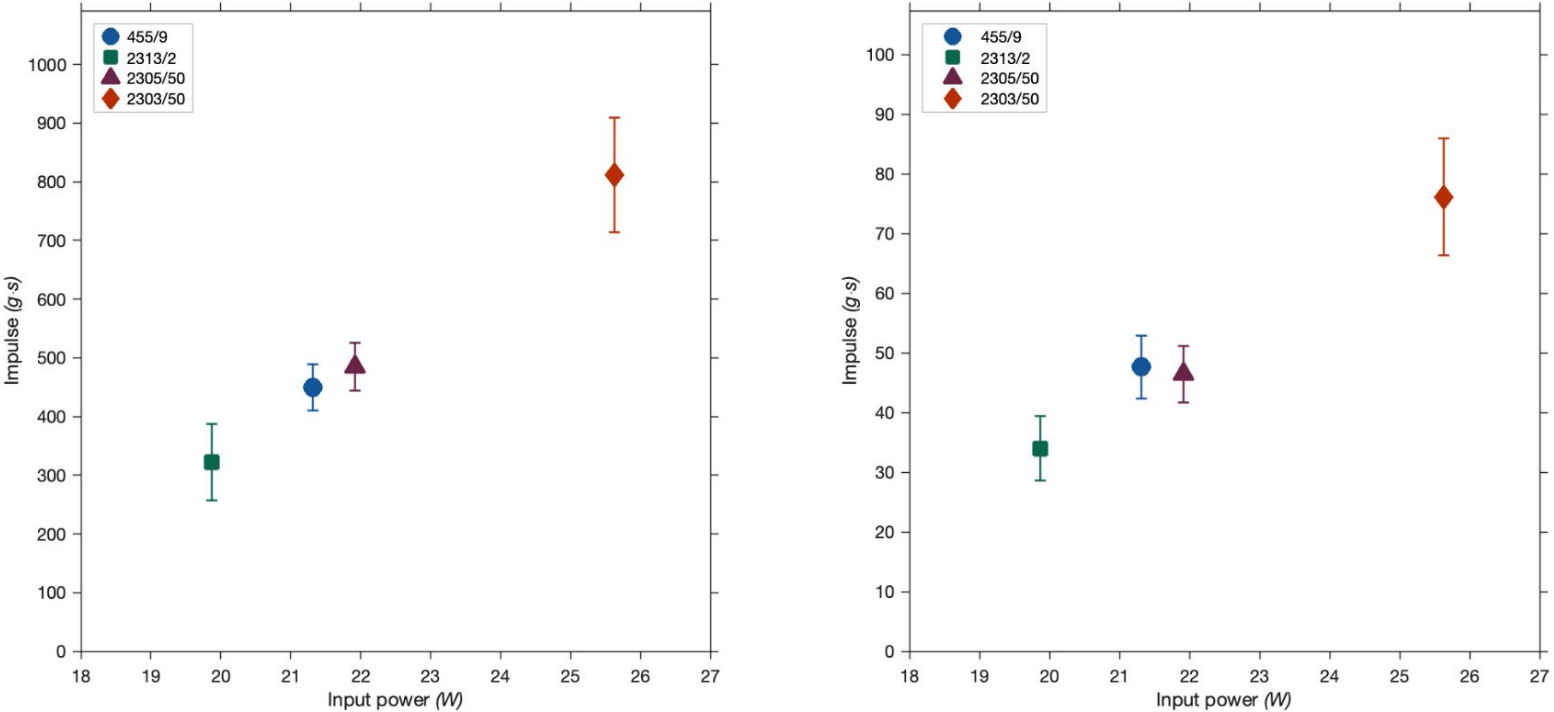

Figure 21: Comparison of thrust impulse to electrical power in both the transient (right) and steady state (left) setting. Error bars represent spread between n trials multiplied by T-estimator for n trials

Theoretical Efficiency of Propellers

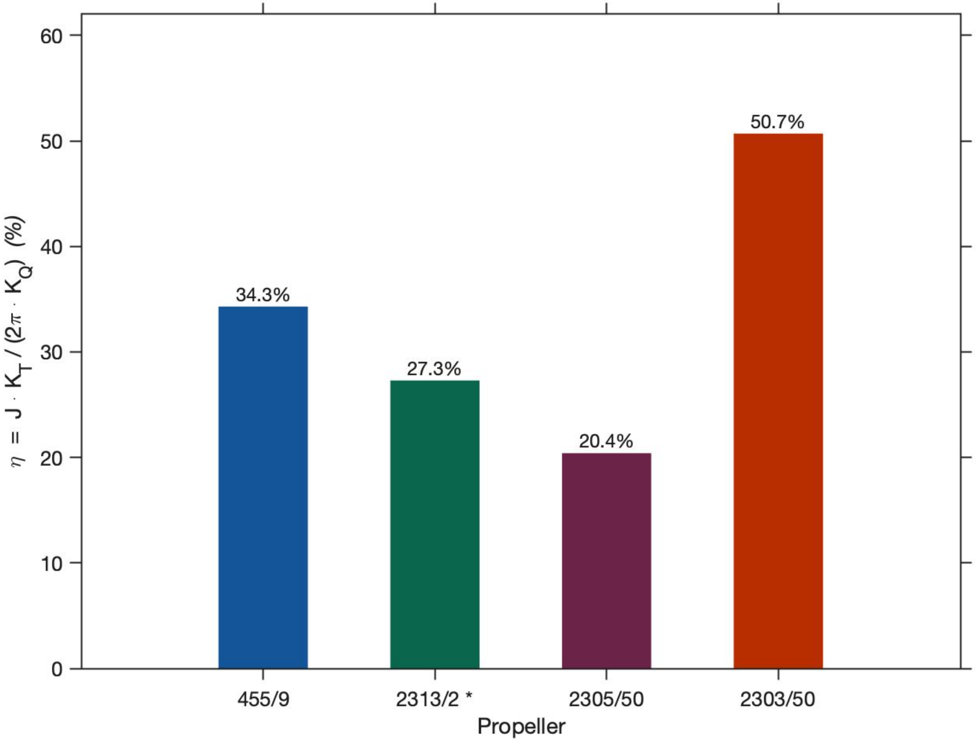

Figure 22: Wageningen B Efficiency approximation of our four propellers at an Advance Ratio of J=0.40

Thrust Vs. Power Compared to Open Water Efficiency of Propellers

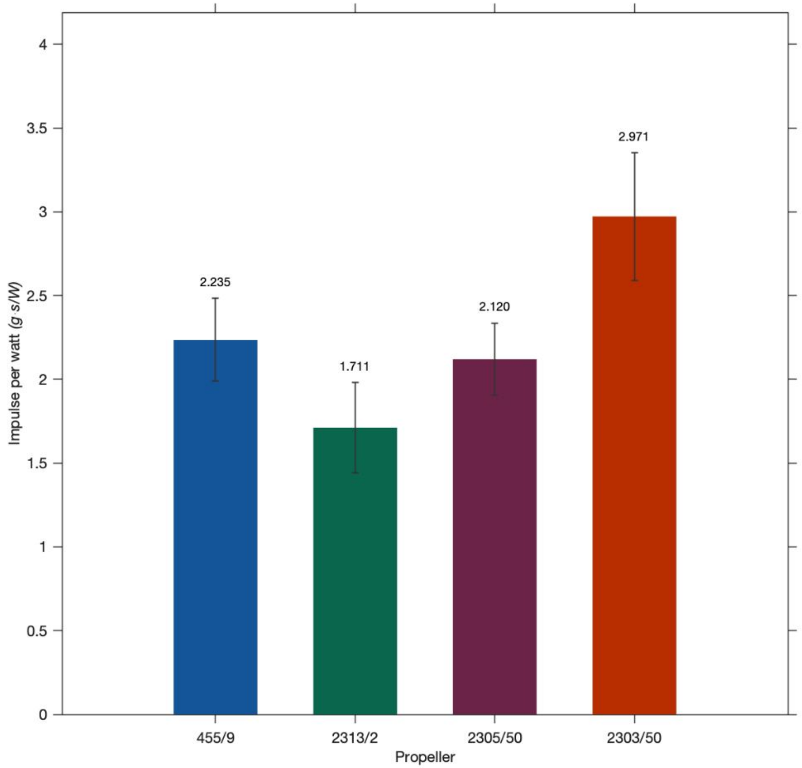

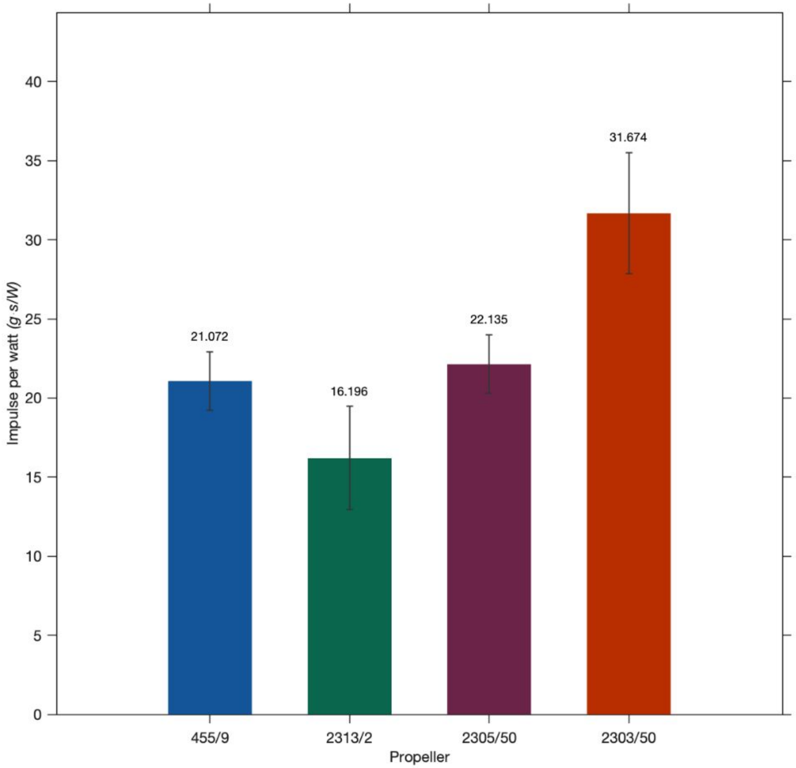

Figure 23: Comparison of thrust to electrical power in both the transient (right) and steady state (left) setting. Error bars represent spread between n trials multiplied by T-estimator for n trials

Discussion and Conclusion

Discussion

Wageningen η evaluates to zero at J = 0 by definition, theoretical and experimental datasets describe different fluid dynamic regimes and rank agreement should not be expected.

At J = 0, KQ is the dominant geometric parameter: with no advance velocity, the motor fights torque load exclusively - lower KQ (2303/50: 0.020) enables faster angular acceleration within the pulse window vs higher KQ (2305/50: 0.165, 2313/2: 0.085)

P/D governs blade angle of attack at J = 0: high P/D (2305/50: 1.6) places blades at a high geometric angle of attack at low RPM during spin-up, driving early stall and torque-dominated loading before useful thrust develops - explains 2305/50's relative underperformance in transient vs its steady state recovery.

The 2305/50 transient/steady-state impulse ratio (~10.4×) is the lowest of the four propellers, high P/D is a spin-up liability that disappears once the flow field is established.

3-blade drawbacks (2313/2): elevated Ae/Ao (0.52) and KQ (0.085) increase wetted drag and added mass - both harmful at J = 0 where there is no advance velocity to recover the induced losses through momentum flux.

2303/50 is optimal across all tested regimes: lowest KQ (0.020), lowest P/D (0.84), moderate Ae/Ao (0.331) - geometrically suited to both rapid spin-up and efficient static disc loading; dominance at J = 0.40 theoretically suggests robustness across the full operating envelope.

Conclusion

2303/50 is the optimal propeller for UUV pulsed position-keeping across both regimes: highest transient at 2.971 g·s/W and highest steady state at 31.674 g·s/W, driven by the lowest KQ (0.020) and lowest P/D (0.84) of the tested set.

At J = 0, KQ is the governing geometric parameter - not P/D or blade count alone - making it the primary selection criterion for propellers operating in pulsed static thrust applications.

During spin-up, the propeller operates against undisturbed fluid with no developed slipstream, resulting in high torque demand and poor thrust output. Once the induced velocity field is fully established at ~0.2s, disc loading efficiency improves dramatically — producing the observed ~10× higher steady-state impulse/watt. This is a fluid dynamic effect, not a measurement artefact.

Wageningen B-Series open water efficiency (evaluated at J = 0.40) correctly identifies 2303/50 as the top performer theoretically, but cannot predict static thrust rank ordering - a new framework characterising bollard-pull efficiency as a function of KQ and spin-up dynamics is needed for pulsed UUV applications.

Areas of Improvement and Ideas for Future Discovery

RPM Measurement: We captured no rotational speed data during trials. Adding a Hall effect sensor would allow direct validation of KQ-based angular acceleration predictions and decouple hydrodynamic from electromechanical losses.

Power Measurement Resolution: Electrical power was read manually from the DC supply display per trial rather than logged continuously. Integrating a current sensor into the DAQ would capture the transient power curve and enable true instantaneous efficiency calculation rather than time-averaged impulse/watt.

Pulse Duration Sweep: Only a single 0.2s transient window was characterised. Testing pulse durations from 0.05s to 1.0s would map the transition from undeveloped to fully-developed slipstream and identify the critical timescale at which steady-state disc loading dominates.

Variable Current Testing: All trials were run at a fixed 3 amps. Testing across a voltage range would reveal whether the KQ-driven performance ranking holds at different motor operating points or is specific to this motor's torque-speed curve.

Citations

1. “Five New Hydrothermal Vents Discovered in the Eastern Tropical Pacific Ocean.” *Woods Hole Oceanographic Institution*, 26 Mar. 2024, https://www.whoi.edu/press-room/news-release/five-new-hydrothermal-vents-discovered-in-the-eastern-tropical-pacific-ocean/

2. “ARV-i Features.” *Boxfish Robotics*, https://www.boxfishrobotics.com/products/arv-i/arv-i-features/. Accessed 7 May 2026.

3. “BlueROV2.” *Blue Robotics*, https://bluerobotics.com/store/rov/bluerov2/. Accessed 7 May 2026.

4. Bernitsas, M. M., et al. *K□, K_q and Efficiency Curves for the Wageningen B-Series Propellers*. University of Michigan, Department of Naval Architecture and Marine Engineering, May 1981.

5. Overmeyer, Austin D., and Preston B. Martin. *The Effect of Laminar Flow on Rotor Hover Performance*. U.S. Army Aviation Development Directorate, NASA Langley Research Center, 2017.

6. Kroll, Thomas Bahati, and Krishnan Mahesh. “A Large-Eddy Simulation Study of Water Tunnel Interference Effects for a Marine Propeller in Crashback Mode of Operation.” *Flow*, 2025, https://doi.org/10.1017/flo.2024.36

Testing Equipment Overview

Part	Number Needed	Cost
Graupner Marine Propellers	4	$24.50
M4 Threaded Rod (300mm)	1	$6.00
DC Motor (1500Rpm, 40-50mA, 12V)	1	Lab Provided
Uline 32 Gallon Bin (27in x 22in or 685mm x 559mm)	1	$33.00
M4 To 3mm DC Motor Shaft Coupler	1	$5.50
1 Kg Load Cell	1	$10.00
DC Power Supply	1	Lab Provided
DAQ Assistant	1	Lab Provided
Multi-Meter	1	Lab Provided
LM741 Operational Amplifier	1	Lab Provided
Extension Cord	1	Lab Provided
Movable Lab Desk	1	Lab Provided

Thank You